Research Article / Review Article FUPRE JOURNAL 9(2):164-178(2025)

FUPRE Journal

of

Scientific and Industrial Research

ISSN: 2579-1184(Print) ISSN: 2578-1129 (Online)

http://fupre.edu.ng/journal

Evaluating the Effects of Cu-Water Nanofluid, Space/Temperature Dependent Heat Source/Sink on Magnetohydrodynamics (MHD) Heat and Mass Transfer Stretching sheet with Buoyancy Forces

***DAMISA, J. S.*[1, *] , *UGBENE, I. J.*[1] , *ABORISADE, Y. J.*[2] , *OKEDOYE, A. M.*[1]**

[1]*Federal University of Petroleum, Department of Mathematics, P.M.B 1221, Effurun, Warri, Delta State, Nigeria*

[2]*Adekunle AjasinUniversity, Department of Mathematical Sciences, P.M.B 001, Akungba Akoko, Ondo State, Nigeria*

ARTICLE INFO

Received: 20/01/2025
Accepted: 20/07/2025

Keywords

Buoyancy effect, Heat and mass transfer, MHD, Nanofluid, volume fraction, Space-temperature dependent heat source/sink, Stretching sheet

ABSTRACT

Magnetohydrodynamics (MHD) heat and mass transfer with nanofluid flow has attracted several authors in science, engineering and several fields of endeavour. Several Newtonian and non-Newtonian fluids experiences friction in the course of motion due to the presence of viscous forces. The flow of Cu-water nanofluid volume fraction with the combine effects of space, temperature dependent heat source/sink and buoyancy forces is considered in this study. The governing equation is transformed from partial differential to ordinary differential using the stream function and the similarity variables and solved numerically using solved numerical using the mathematical package called the Mid-point Richardson extrapolation code in MAPLE 2021. Hence, results are shown in tables and graphs for various increasing values of the governing parameters. It is revealed from the result of the study that the increase in the second-grade parameter (α) results in the increase of the fluid velocity, The increasing function of the volume fraction (φ) brings about the increase in the fluid motion and in the temperature of the fluid at free stream, the increase in the space and temperature dependent heat source/sink parameters A and B respectively result to the increase in the of the temperature at the free stream and decrease in the concentration of the fluid and the increase in the yields result to increase in the motion, temperature and concentration of the fluid.

1. INTRODUCTION

Magnetohydrodynamics (MHD) is the study fluid conduction electrically in the presence of magnetic field. It is also referred to as magnetofluid mechanics or hydromagnetics which is described generally as any means of electrically conducting fluid flow by magnetic field. This study was first introduced by Hannes Alven. (Sathy *etal* 2022). Any means of electrically conducting fluid flow by magnetic field. Magnetic induction is the production of an electromotive force or voltage across an electrical conductor due to its dynamic interaction with a magnetic field as discussed by Animasaun and Sandeep (2016). The central focus of the MHD is that fluid conducted is supported by magnetic field. The presence of magnetic field produces the forces that acts upon the fluid. The fundamental concept of the magnetohydrodynamics (MHD) is the fact that magnetic field can induce currents in the flow of conductive fluid, this will in turn produce forces on the fluid in motion and alter the magnetic field itself, Mohsen and Davood (2016). The MHD system is seen as a converter working on the principle of link between a magnetic field and the electrically

*Corresponding author, e-mail:damisa.john@fupre.edu.ng
DIO

conducting fluid. This was first initiated by Faraday at the start of the 19th century. (Vyacheslav chernyshev 2010). From various literatures so far, it is discovered that MHD focuses on the fluid conduction. This is also applicable in ionic solutions. The potential difference applied across two electrode immersed in an ionic, aqueous solution in an appropriate situation, electrochemical reaction occur at the electrode surface and ion motion takes place in the chemical composition. The ionic transport is viewed as electric current under the microscope. The electric current interact with the magnetic field present in the system to produce a body force and induce fluid motion. (Shizhi *etal* 2012). The transfer of energy and species plays a large considerable role in the field of sciences and engineering. This has been a topic of great interest amongst researchers across the world. This is so because of its wide range of application and uses in various industries as it plays a vital and significant roles in the production processes. Okedoye *etal*. (2022) examined the two dimensional dissipative non-slip MHD flow of Arrhenius chemical reaction with variable properties. In the study, viscous fluid flows along a fixed impermeable wall or rigid surface or an immersed body with an essential condition that the velocity at any point on the wall or other fixed surface is zero. It is discovered that even at a low Reynold number, nonlinear heat and mass transfer flow occur close to *x*-axis boundary. The application of the study of heat and mass transfer also cut across the cooling of metallic plate, oceanography and the movement of biological fluids. Ramanahalli *etal*. (2021) analysed the impact of binary chemical reaction and activation energy on heat and mass transfer of marangoni driven boundary layer flow of a non-Newton nanofluid, the study reveals that the increase in the value of the marangoni number enhances the velocity gradient and reduces the heat transfer and the increase in the porosity parameter enhances the heat transfer and reduces the velocity gradient of the fluid flow.

A mixed convective flow of fluid is referred to as a process where both natural convection force and force convection mechanism simultaneously act on the movement of fluid. This can happen when a fluid is subjected to a combine force. The natural convection is the buoyancy-driven flow and the force convection mechanism is the externally imposed force that causes the flow fluid. The entire behaviour of the fluid flow can be determined by the strength of the two forces interacting to cause a flow in the fluid. Okedoye and Akinrinmade (2017) analysed the MHD mixed convection heat and mass transfer flow from vertical surfaces in poros media with soret and dufour effects. Hatem *etal.*(2022), reported the analysis of mixed convection on two-phase nanofluid flow past a vertical plate in Brinkman-extended darcy porous medium with nield condition. A steady flow near an impermeable vertical flat plate subjected to mixed convection emended in a porous medium filled with nanofluid flowing with non-uniform free-stream velocity was considered. It is revealed here that the increase in the porosity parameter causes a decline in the velocity of the fluid and that in buoyancy aiding flow and buoyancy opposing flow, there is an enhancement in the temperature and concentration of the fluid flow. Ahmad *etal.*(2022) examined the mixed convective flow of an electrically conducting viscoelastic fluid past a vertical nonlinearly stretching sheet. The research work took into consideration the viscoelastic fluid flowing in mixed convection two dimensional MHD flow across a stretching sheet. The *x*-axis is drawn along the continuously extending surface and faces forward but parallel to the *y*-axis and the sheet is subjected to a perpendicular magnetic field. The research shows that the increase in the magnetic parameter leads to the enhancement of the distribution of the viscoelastic fluid temperature and decline in the temperature gradient of at away from the free stream. Also, the increase in the radiation parameter causes the increase in the temperature distribution and the associated thermal layer.

Heating and cooling procedure is a vital process in several industrial production. This process takes place in petrochemical industries, textile production industries, paper industries, chemical industries, vehicular cooling process in the transportation industry and cooling systems in buildings are some of the numerous applications of heat transfer. In all of these applications, the thermal conductivity of heat transfer plays a very significant role in sustaining energy-efficient heating system. Hence, there is the need of production industries to create or invent a stronger and advanced heat transfer characterized with higher thermal conductivities. Here, the concept of volume

fraction of nanofluid is required. The volume fraction of nanofluid is described as the ratio of nanoparticles volume over the total volume of the entire nanofluid. Kannaiyan *et al.* (2017) revealed in his work that fluids containing nanoparticles provides a way to attain heat transfer enhancement as a result of their thermophysical properties and their high thermal conductivity. However, when nano-particles are added to the fluid, other thermophysical properties of the fluid like viscosity and thermal conductivity are influenced. To enable the usage of nanofluids in practical applications, the extent of the thermal conductivity and viscosity increase of nanofluids with respect to pure fluids should be thoroughly investigated. Choi *et al.* (1995) reported that the nanofluids were proved to have high thermal conductivities compared to those of currently used heat transfer fluids, leading to enhancement of heat transfer. Kwak and Kim (2005) reported the variations in zero shear viscosity for different volume fractions and compared the obtained results with present models. They also presented the variation of nanofluid viscosity with various shear rates for nanofluid diverse volume fractions. The effect of temperature, nanoparticle size, and nanoparticles volume fraction on thermal conductivity was experimentally examined by Chon *et al.* (2005) and they showed that nanofluid thermal conductivity is also affected by temperature, volume fraction of nanoparticles, and nanoparticle size. Furthermore, Nguyen *et al.* (2007) and Angue Minsta *et al.* (2009) studied the effect of nanoparticles concentration, nanoparticles size on nanofluids viscosity under a wide range of temperatures experimentally. They revealed that temperature deflates the viscosity especially for high concentration of nanoparticles. In view of all these facts, such physics cannot be neglected and the dependence of nanofluid properties on temperature, volume fraction of nanoparticles, must be taken into account in order to predict the correct role of nanoparticles on heat transfer enhancement. This reality motivated Abu-Nada (2009) to discuss the effects of viscosity and thermal conductivity of Al_2O_3–water nanofluid. More recently, Liu *et al.* (2011) examined the thermal conductivity relative to nanofluid for different copper oxide nanofluid volume fractions.

The space, temperature dependent heat source/sink is also refer to as the non-uniform heat source/sink which is expressed in energy equation. In considering thermodynamics, this is described as the energy stored that can absorb certain amount of heat without significantly altering the temperature of the fluid. Several researcher has evaluated the effects of the space, temperature dependent heat source/sink. Bijjanal *et al* (2011) examined the boundary layer flow of an unsteady dusty fluid and heat transfer over a stretching sheet with non-uniform heat source/sink. The study was focused on the effects of magnetic field on unsteady boundary layer flow and heat transfer of a dusty fluid over a stretching sheet in the presence of non-uniform heat source/sink. The temperature distribution is evaluated with variable wall temperature (VWT) and variable heat flux (VHF) temperature boundary conditions. From the study, it is revealed from the study that the various physical parameters such as magnetic parameter decreases the velocity of the fluid flow when there is an increase and the temperature decreases when there is an increase in the prandtl number (Pr) in both cases of (VWT) and (VHF). Also, Anjali devi and Agneeshwari (2019) studied the effects of non-uniform heat generation/absorption and radiation on hydromagnetic dissipative flow over a porous nonlinear stretching surface with heat and mass fluxes.

Motivated by the findings and applications mentioned above, the main aim of this study is to Evaluate the Effects of Cu-Water Nanofluid, Space/Temperature Dependent Heat Source/Sink on Magnetohydrodynamics (MHD) Heat and Mass Transfer Stretching sheet with Buoyancy Forces. The research is based on a combined analysis of the effects thermophysical properties of copper-water nanofluid, the mixed convective heat and mass transfer MHD, the impact of the thermophoresis and the Brownian motion, the suction/injection effect with the non-uniform heat source/sink and pressure gradient effect on the flow field. This is numerically analysed using the mathematical package package known as the Mid-point Richardson extrapolation code in MAPLE 2021.

2. MATHEMATICAL ANALYSIS

Consider a two dimensional, unsteady, laminar, incompressible second-grade nanofluid flow past a surface. The fluid is driven by a constant pressure gradient and buoyancy forces. We also consider the *x*-

component equation along the direction of the fluid flow and the *y*-component equation perpendicular to it. The Reynolds number R tends to infinity, or the kinematic viscosity υ tends to zero, of a limiting form of the equations of motion, different from that obtained by putting $\upsilon = 0$ in the first place. A solution of these limiting equations may then reasonably be expected to describe approximately the flow in a laminar boundary layer for which R is large but not infinite. This is the basis of the classical theory of laminar boundary layers. The nanofluid under consideration in this study has water (H_2O) as the base fluid with a nanoparticle of Copper (Cu). Taking the dynamic viscosity(μ_{nf}), effective density (ρ_{nf}), thermal conductivity (α_{nf}) and the heat capacity $(\rho C_p)_{nf}$ into account. It is assumed that the base fluid and the nanoparticles are in equilibrium and no slip occurs between them. Hence, the full equation of motion for the two-dimensional equation is equations (1) to (5);

$$\frac{\partial u}{\partial x}+\frac{\partial v}{\partial y}=0 \tag{1}$$

$$\frac{\partial u}{\partial t}+u\frac{\partial u}{\partial x}+v\frac{\partial u}{\partial y}=-\frac{1}{\rho_{n_f}}\frac{\partial p}{\partial x}+\frac{\mu_{nf}}{\rho_{nf}}\frac{\partial^2 u}{\partial y^2}+\frac{\alpha_1}{\rho_{n_f}}\tau_1-\frac{\sigma\mu B_o^2(x)}{\rho_{n_f}k_1}(u-U) \mp\frac{g}{\rho_{n_f}}\left(\frac{k_1}{\upsilon}\right)|\hat{u}|(u-U)+\frac{g\beta_\tau}{\rho_{n_f}}(T-T_\infty)+\frac{g\beta_c}{\rho_{n_f}}(C-C_\infty) \tag{2}$$

$$\frac{\partial v}{\partial t}+u\frac{\partial v}{\partial x}+v\frac{\partial v}{\partial y}=-\frac{1}{\rho_{n_f}}\frac{\partial p}{\partial y}+\frac{\mu_{nf}}{\rho_{nf}}\frac{\partial^2 u}{\partial y^2}+\frac{\alpha_1}{\rho_{n_f}}\tau_2-\frac{\sigma\mu B_o^2(x)}{\rho_{n_f}k_1}(u-U) \tag{3}$$

$$\frac{\partial T}{\partial t}+u\frac{\partial T}{\partial x}+v\frac{\partial T}{\partial y}=\frac{\alpha_{nf}}{(\rho C_p)_{nf}}\frac{\partial^2 T}{\partial y^2}-\frac{1}{(\rho C_p)_{nf}}\frac{\partial q_r}{\partial y}+N_{nf}\left[D_B\frac{\partial T}{\partial y}\frac{\partial C}{\partial y}+\frac{D_T}{T_\infty}\left(\frac{\partial T}{\partial y}\right)^2\right]+\frac{\mu_{nf}}{(\rho C_p)_{nf}}\left(\frac{\partial u}{\partial y}\right)^2+\frac{q'''}{(\rho C_p)_{nf}} \tag{4}$$

$$\frac{\partial C}{\partial t}+u\frac{\partial C}{\partial x}+v\frac{\partial C}{\partial y}=\frac{D_m k_T}{\rho_{n_f}}\frac{\partial^2 C}{\partial y^2}+\frac{R_A}{\rho_{n_f}}-\frac{1}{\rho_{n_f}}\frac{\partial}{\partial y}\left((C-C_\infty)V_T\right) \tag{5}$$

$$\left.\begin{aligned}\tau_1&=\frac{\partial u}{\partial x}\frac{\partial^2 u}{\partial y^2}+u\frac{\partial^3 u}{\partial y^2\partial x}-\frac{\partial u}{\partial y}\frac{\partial^2 u}{\partial y\partial x}+v\frac{\partial^3 u}{\partial y^3}\\ \tau_2&=\frac{\partial v}{\partial x}\frac{\partial^2 v}{\partial y^2}+u\frac{\partial^3 v}{\partial y^2\partial x}-\frac{\partial v}{\partial y}\frac{\partial^2 v}{\partial y\partial x}+v\frac{\partial^3 v}{\partial y^3}\end{aligned}\right\} \tag{6}$$

It is assumed that the radiation heat flux is to be presented in the form of a unidirectional flux in the y direction. Using the Roseland approximation in Shankar and Eshetu (2015), the radiative heat transfer and the Roseland approximation for diffusion, the expression for the radiative heat flux q_r can be given as;

$$q_r=\left(\frac{-4\sigma}{3k_s}\right)\left(\frac{\partial T^4}{\partial y}\right) \tag{7}$$

In Equation (7), the parameters σ and k_s represent the Stefan Boltzmann constant and the Roseland mean absorption coefficient, respectively. Now on assuming that the temperature differences within the fluid flow are sufficiently small, T^4 in Equation (7) can be expressed as a linear function of T_∞ ' using the Taylor series expansion. The Taylor series expansion of T^4about T_∞ , after neglecting the higher order terms, takes the form

$$T^4\cong 4T_\infty^3 T-3T_\infty^4 \tag{8}$$

Hence, substituting Equation (7) into Equation (8) and simplify, we have;

$$q_r=\left(\frac{-4\sigma}{3k_s}\right)\left(\frac{\partial\left(4T_\infty^3 T-3T_\infty^4\right)}{\partial y}\right),\ q_r=\left(\frac{-4\sigma}{3k_s}\right)\left(4T_\infty^3\frac{\partial T}{\partial y}\right)$$

$$q_r=-\frac{16\sigma T_\infty^3}{3k_s}\frac{\partial T}{\partial y} \tag{9}$$

We employed chemical reaction of Arrhenius type of the *1st* order irreversible reaction given by;

$$R_A=k_r^2(T-T_\infty)^r\exp\left(-\frac{E_a}{R_G T}\right)(C-C_\infty) \tag{10}$$

Where k_r^2 is the reactivity of chemical

reaction defined by frequency of collision ω and orientation factor p as $k_r = k_r(\omega, p) = \omega p$, R_G is the universal gas constant?

In the same analysis, non-uniform heat source/sink (q''') and thermo-phoretic velocity (V_T) are given by

$$q''' = \left(\frac{\kappa u_w(x)}{xv}\right)\left[\frac{A^*(T_w - T_\infty)}{bx}(u - U) + B^*(T - T_\infty)\right] \quad (11)$$

$$V_T = \frac{k'v}{\tau}\frac{\partial T}{\partial y} \quad (12)$$

Using equations (6) – (12), the x-momentum equations (2), y-momentum equation (3), the energy transfer equation (4) and the mass (species) transfer equation (5) becomes;

$$\frac{\partial u}{\partial t} + u\frac{\partial u}{\partial x} + v\frac{\partial u}{\partial y} = -\frac{1}{\rho_{n_f}}\frac{\partial p}{\partial x} + \frac{\mu_{nf}}{\rho_{nf}}\frac{\partial^2 u}{\partial y^2} - \frac{\sigma\mu B_o^2(x)}{\rho_{n_f}k_1}(u - U) + \frac{\alpha_1}{\rho_{n_f}}\left(\frac{\partial u}{\partial x}\frac{\partial^2 u}{\partial y^2} + u\frac{\partial^3 u}{\partial y^2 \partial x} - \frac{\partial u}{\partial y}\frac{\partial^2 u}{\partial y \partial x} + v\frac{\partial^3 u}{\partial y^3}\right) \mp \frac{g}{\rho_{n_f}}\left(\frac{k_1}{v}\right)|\hat{u}|(u - U) + \frac{g\beta_\tau}{\rho_{n_f}}(T - T_\infty) + \frac{g\beta_c}{\rho_{n_f}}(C - C_\infty) \quad (13)$$

$$\frac{\partial v}{\partial t} + u\frac{\partial v}{\partial x} + v\frac{\partial v}{\partial y} = -\frac{1}{\rho_{n_f}}\frac{\partial p}{\partial y} + \frac{\mu_{nf}}{\rho_{nf}}\frac{\partial^2 v}{\partial y^2} - \frac{\sigma\mu B_o^2(x)}{\rho_{n_f}k_1}(v - U) + \frac{\alpha_1}{\rho_{n_f}}\left(\frac{\partial v}{\partial x}\frac{\partial^2 v}{\partial y^2} + u\frac{\partial^3 v}{\partial y^2 \partial x} - \frac{\partial v}{\partial y}\frac{\partial^2 v}{\partial y \partial x} + v\frac{\partial^3 v}{\partial y^3}\right) \quad (14)$$

$$\frac{\partial T}{\partial t} + u\frac{\partial T}{\partial x} + v\frac{\partial T}{\partial y} = \frac{\alpha_{nf}}{(\rho C_p)_{nf}}\frac{\partial^2 T}{\partial y^2} - \frac{1}{(\rho C_p)_{nf}}\frac{16\sigma T_\infty^3}{3k_s}\frac{\partial^2 T}{\partial y^2} + N_{nf}\left[D_B\frac{\partial T}{\partial y}\frac{\partial C}{\partial y} + \frac{D_T}{T_\infty}\left(\frac{\partial T}{\partial y}\right)^2\right] + \frac{\mu_{nf}}{(\rho C_p)_{nf}}\left(\frac{\partial u}{\partial y}\right)^2 + \frac{D_m k_{nf}}{\rho_{n_f}}\frac{\partial^2 C}{\partial y^2} + \frac{\sigma\beta_0^2}{(\rho C_p)_{nf}}u^2 + \frac{1}{(\rho C_p)_{nf}}\left(\frac{\kappa u_w(x)}{xv}\right)\left[\frac{A^*(T_w - T_\infty)}{bx}(u - U) + B^*(T - T_\infty)\right] \quad (15)$$

$$\frac{\partial C}{\partial t} + u\frac{\partial C}{\partial x} + v\frac{\partial C}{\partial y} = \frac{D_m k_T}{\rho_{n_f}}\frac{\partial^2 C}{\partial y^2} + \frac{1}{\rho_{n_f}}k_r^2(T - T_\infty)^r \exp\left(-\frac{E_a}{R_G T}\right)(C - C_\infty) - \frac{k'v}{\tau\rho_{n_f}}\frac{\partial^2 T}{\partial y^2} \quad (16)$$

Where u and v are the velocity component in the x and y direction respectively. p is the fluid pressure. A wall is located in the plane $y = 0$. α_1 is the second-grade fluid parameter (also known as the normal stress moduli), τ_1 and τ_2 are the second-grade model on the x and y momentum equations respectively, k_1 is the permeability of the porous medium, T is the temperature of the nanofluid, C is the concentration of the nanofluid, T_∞ is the ambient temperature, C_∞ is the ambient concentration, q_r is the radiative heat flux, D_m is the mass diffusivity, k_T is the thermal diffusion ratio, according to Buongiorno (2006), D_B is the Brownian diffusion coefficient, D_T is the thermophoretic diffusion coefficient and N_{nf} is the Buongiorno's parameter expressed as

$$N_{nf} = \frac{(\rho C_p)_s}{(\rho C_p)_f} \quad (17)$$

Then according to Shankar and Eshetu (2014), the dynamic viscosity(μ_{nf}), effective density(ρ_{nf}), thermal conductivity (α_{nf}) and the heat capacitance of the nanofluid $(\rho C_p)_{nf}$ are expressed as;

$$\left.\begin{aligned} \mu_{nf} &= \frac{\mu_f}{(1-\phi)^{2.5}} \\ \rho_{nf} &= (1-\phi)\rho_f + \phi\rho_s \\ \alpha_{nf} &= \frac{\kappa_{nf}}{(\rho C_p)_{nf}} \\ (\rho C_p)_{nf} &= (1-\phi)(\rho C_p)_f + \phi(\rho C_p)_s \end{aligned}\right\} \quad (18)$$

The thermal conductivity of nanofluid of a spherical Nanoparticle according to Shankar and Eshetu (2014) is given as:

$$k_{nf} = k_f\left[\frac{k_s + 2k_f - 2\emptyset(k_f - k_s)}{k_s + k_f - \emptyset(k_f - k_s)}\right] \quad (19)$$

$$A^* = (T_w - T_\infty), B^* = (C_w - C_\infty) \quad (20)$$

Where $A^*, B^* > 0$ the coefficients of

space and temperature dependent heat are source/sink respectively is defined as;
The appropriate initial and boundary conditions relevant to the problem are analysed as;

$$t \le 0: u = U_w, v = v_w(t), T = T_w, C = C_w \; \forall y$$
$$t > 0: \begin{cases} u = U_w, v = 0, \begin{cases} T = T(x,t) \\ -k\dfrac{\partial T}{\partial y} = q_f(x,t) \end{cases}, C = C_w, y = 0 \\ u \to U_\infty(x,t), \dfrac{\partial u}{\partial y} \to 0, T \to T_\infty, C \to C_\infty \; as \; y \to \infty \end{cases} \quad (21)$$

Where U_w is the plate characteristic velocity defined as;

$$U_w(x,t) = \frac{ax}{1-\lambda t} \quad (22)$$

The stream velocity is given by

$$U_\infty(x,t) = \frac{cx}{1-\lambda t} \quad (23)$$

At free stream,

$$u \to U, T \to T_\infty, , C \to C_\infty \quad (24)$$

While at time $y = 0$, the suction/blowing is a function free stream given as

$$v(t,0) = v_w(t) = -\frac{v_0}{\sqrt{1-\lambda t}} \quad (25)$$

$v_0(>0)$ is the suction velocity and $v_0(<0)$ is the blowing velocity.

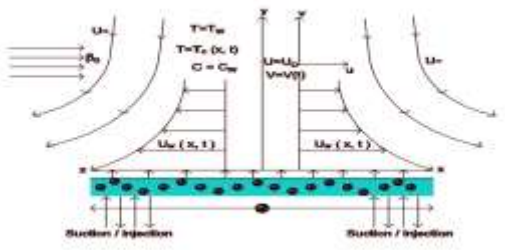

Fig. 1.Physical configuration.

The transformed governing equations with its boundary/initial conditions with the special cases becomes;

$$f''' + \phi_1\left(G(x) + \frac{Ha}{\phi_2}(f'-1) + \alpha_0\{2f'f''' - (f'')^2 - ff'^v\} - \frac{\eta}{2}f'' - f' + (f')^2 + ff'' \mp \frac{Fs}{\phi_2}(f'-1) + Gr(Gr_N g + h)\right) = 0 \quad (26)$$

$$\left(1+\frac{4R}{3}\right)g'' + Pr\phi_3\frac{k_f}{k_{nf}}\left(Nbg'h' + Ntg'^2 - g' + fg' + \frac{Ec}{\phi_4}f''^2 + [A^*(f'-1) + B^*g]\right) = 0 \quad (27)$$

$$\frac{1}{Sc}h'' - \frac{\rho_{n_f}}{\rho_f}\left(\frac{\lambda}{a}\frac{\eta}{2} - f\right)h' + \Omega(g)^r \exp\left(\frac{g}{1+\epsilon g}\right)h - Srg'' = 0 \quad (28)$$

With the Boundary/Initial conditions

$$f' = 1, f = S_0, g = 1, h = 1 \; \forall y \; at \; time \; t \le 0$$
$$f' \to \frac{c}{a}, f'' \to 0, g \to 0, h \to 0 \; as \; y \to \infty \; at \; t > 0 \quad (29)$$

Prime denotes differentiation with respect to η, $Pr = \frac{\upsilon_f}{\alpha_f}$ (Prandtl number), $\gamma = \frac{k_r^2 L T_\infty (C_w - C_\infty)}{U}(\epsilon)^{r-1}$ is the chemical reaction parameter, $k_1 = \frac{\upsilon_f}{bk}$ (Porous medium parameter), $M = \frac{\sigma\beta_0^2}{b\rho_f}$ (magnetic parameter), $Sr = \frac{k'\nu L T_\infty (T_w - T_\infty)}{\rho_{n_f}\tau}$ is the Soret number, $Sc = \frac{\rho_{n_f} U\delta^2}{D_m L}$ is the Schmidt number, $R = \frac{4\sigma^* T_\infty^3}{k^* k}$ (Radiation parameter), $Ec = \frac{u_w{}^2}{(C_p)_f(T_w - T_\infty)}$(Eckert number), $\alpha_0 = \frac{\alpha_1}{\rho_f}$ is the elastic parameter, α_1 is the second grade parameter (also known as the normal stress moduli), $Ha = \frac{\sigma\beta_0^2}{\rho_f a k_1}$ is the Hartman number, $Re = \frac{\upsilon_f}{\rho_f \mu_f}$ is the Reynolds number, $Fs = \frac{g\upsilon_f}{\rho_f}\left(\frac{k_1}{\upsilon}\right)|\hat{u}|$ is the Darcy-Forcheimer number, $Gr = \frac{g\beta_T(T_w - T_\infty)}{\rho_f}$ is the grashof number (Buoyancy due to temperature) and $Gr_N =$

$\frac{g\beta_C(C_w-C_\infty)}{\rho_f}$ is the ratio of grashof number (Buoyancy due to concentration), $N=\frac{1-\lambda t}{ax}$ is the inverse of the dimensionless parameter in constant interaction with the flow of the nanofluid. $Nb=\frac{N_{nf}D_B(C_w-C_\infty)}{(C_p)_f}$ is the Brownian motion parameter, $Nt=\frac{N_{nf}D_T}{(C_p)_f T_\infty}$ is the thermophoresis parameter, $\epsilon=\frac{R_G T_\infty}{E_a}$ is the activation energy parameter.

$\phi_1=(1-\emptyset)^{2.5}\left(1-\phi+\phi\left(\frac{\rho_s}{\rho_f}\right)\right)$, $\phi_2=1-\phi+\phi\left(\frac{\rho_s}{\rho_f}\right)$, $\phi_3=1-\phi+\phi\left(\frac{(\rho c_p)_s}{(\rho c_p)_f}\right)$, $\phi_4=(1-\phi)^{2.5}\left(1-\phi+\phi\left(\frac{(\rho c_p)_s}{(\rho c_p)_f}\right)\right)$ To simply the above equation, let $\phi_1=(1-\phi)^{2.5}\left(1-\phi+\phi\left(\frac{\rho_s}{\rho_f}\right)\right)$ is the product of the nanofluid viscosity with the ratio of the nanofluid base fluid and nanoparticles.

Rate of flow at the wall: Physical quantities of engineering interest in the flow are skin friction coefficient C_f and Nusselt number Nu and local Sherwood number Sh defined respectively as;

$C_f=\frac{2\tau_w}{\rho_f u_w^2\sqrt{Re_x}}$, $\tau_w=\mu_{nf}\left(\frac{du}{dy}\right)_{y=0}$, $Nu=-\frac{xq_w}{k_f(T-T_\infty)}$, $q_w=k_{nf}\left(\frac{dT}{dy}\right)_{y=0}$ and $Sh=-\frac{q_w}{D_B(C_w-C_\infty)}$,

$$q_w=D_B\frac{dC}{dy}$$

$C_f=\frac{2f''(0)}{(1-\phi)^{2.5}}$, $Nu=\frac{k_{nf}}{k_f}\left(1-\frac{4R}{3}\right)g'(0)$,

$$Sh=\frac{1}{Sc}h'(0) \qquad (30)$$

Table 1: *The thermophysical properties of water (H_2O), copper (Cu) and Alumina (Al_2O_3) Motsumi and Makinde (2012).*

	PROPERTIES		
PHYSICAL QUANTITIES	$\rho(Kg/m^2)$	$C_p(J/Kgk)$	$K(W/mk)$
Pure water (H_2O)	997.1	4179	0.613
Copper (Cu)	8933	385	400

3. RESULTS AND DISCUSSION

The transformed governing equation in the form of ODE (26), (27), (28) with the boundary/initial conditions (29) associated with this study is solved and evaluated using the Rchardson extrapolation techniques which is executed by MAPLE2023. The Richardson extrapolation techniques is a sequence acceleration method used to improve the rate of convergence of sequence which was introduced by Lewis Fry Richardson in the early 20th century. It is a mathematical software that combines complex mathematical equation with interface that makes it easy to analyse, explore, visuallize and solve mathematical problems. It is a powerful tool for both symbolic and numerical mathematical computation. Hence, this section presents the impacts of the various governing parameters like Prandtl number (Pr), chemical reaction parameter (γ), Porous medium parameter (k_1), magnetic parameter (M), Soret number (Sr), the Schmidt number (Sc), Radiation parameter (R), Eckert number (Ec), elastic parameter (α_0), the second grade parameter (also known as the normal stress moduli (α_1), the Hartman number Ha, the Darcy-Forcheimer number (Fs), the grashof number (Buoyancy due to temperature) (Gr), the ratio of grashof number (Buoyancy due to concentration) (Gr_N), Brownian motion parameter (Nb), the thermophoresis parameter (Nt) and the volume fraction (ϕ).

Table 2: *Nanofluid Volume Fraction effect on the flow field*

Parameter(ϕ)	C_f	Nu	Sh
0.0	0.555104	0.614044	-0.484875
0.2	2.113220	1.435831	-1.051900
0.4	1.943455	0.710324	-1.524882

Table 3: Variation of reactivity parameter(Ω), reaction index (r), second grade fluid parameter (α_0), unsteadiness parameter (β) with wall rate transfer and sheet stretching parameter

Parameters ($\Omega, r, \alpha_0, \beta$ *and* λ) when $\phi = 0.2$	C_f	Nu	Sh
	Nanofluid	Nanofluid	Nanofluid
$\Omega = 0.03$	2.130257	1.508161	-1.332235
$\Omega = 0.05$	2.135968	1.512947	-1.130285
$\Omega = 0.07$	2.141852	1.517924	-0.923463
r =0.0	2.134357	1.511550	-1.183502
r =1.0	2.135538	1.512808	-1.163114
r =2.0	2.137471	1.514889	-1.131511
α_0 =0.3	2.135146	1.512137	-1.149599
α_0 =0.4	1.789960	0.720487	-1.256043
α_0 =0.5	1.548841	0.427346	-1.280995
$\lambda = 0.2$	2.135146	1.512137	-1.149599
$\lambda = 0.4$	2.120730	0.775143	-1.467782
$\lambda = 0.6$	2.101336	0.474465	-1.727259

3.1 Discussion

VELOCITY FIELD

The velocity field constitute every motion of fluid within specific regions or movement of fluid within a specific region over a surface. This is characterized by velocity vector at every point in the surface. The various governing parameters directly affects the movement of the fluid under consideration at some point in the region. Figure 2 depict the effects of the volume fraction parameter (ϕ) on the velocity field. The volume fraction of a nanofluid is the ratio of nanoparticles volume over the total volume of the nanofluid. It is observed from the figure that the increase in the volume fraction parameter leads to an increase in the velocity field of the fluid. Figure 3 shows the effect Hartman (Ha) number on the motion of fluid. This brings about the equilibrium between the Lorentz forces and the viscous forces in diffusive magnetic layer at an interface between materials with difference electric properties in conjunction with magnetic field which has the tendencies of slowing down the motion of fluid. This is observed in figure 3 as the increase in the Hartman number (Ha) results to the decrease in the movement of the velocity field. Figure 4 indicate the impact of Darcy Foreichemer parameter (Fs) on velocity field. It is observed from the figure that the velocity of the fluid decreases with an increase in the Darcy Foreichemer parameter(Fs). Figure 5 shows the effect of Buoyancy Parameter (Gr) on velocity field. It is observed from the figure that increase in the buoyancy parameter causes a n increase in the fluid away from wall, but shows a bit reduction in the velocity of the fluid at the free stream. Figure 6 indicates the effect of Pressure Gradient parameter (G) on velocity field. The pressure gradient is described as the rate of change of pressure with respect to distance. This usually brings about the increase in the motion of fluid in a specific direction. From the figure, it is seen that the increase in the pressure gradient parameter brings about the increase in the velocity of the fluid flow.

TEMPERATURE FIELD

The temperature field expresses the ratio of the environmental and surface temperature difference of a body to the difference between the environmental temperature and the average integral volume temperature. The parameters under consideration plays a vital role in the control of temperature in the temperature field. Figure 7 shows the effect of volume fraction (ϕ) on Temperature field. It is observed from the figure that there is a decrease in the temperature away from the wall and an increase in the temperature at the free stream when there is an increase in the volume fraction parameter. Figure 8 depict the effect of Hartman Number (Ha) on Temperature Field. From the figure, it is observed from the figure that

the increase in the Hartman number show little increase in the temperature at some point and shows no significant effect at other point. Figure 9 indicates the effect of Thermophoresis parameter (Nt) on Temperature field. The figure shows a significant increase in the temperature at all point when there is an increase in the Thermophoresis parameter. Figure 10 shows the effect of Buoyancy parameter (Gr) on Temperature field. It is observed from the figure that there is increase in the temperature of the fluid at all point when there is an increase in the Buoyancy parameter. Figure 11 shows the effect of radiation parameter (R) on Temperature field. It is revealed from the figure that the increase in the radiation parameter leads to the decrease in the temperature of the fluid away from the wall and shows a little increase in the temperature at the free stream. Figure 12 symbolizes the effect of Eckert Number (Ec) on Temperature field. The Eckert Number is used to characterize the heat transfer dissipation. From the figure, it is observed that the increase in the Eckert Number parameter shows little or no significant effect at the wall, but yields a significant increase away from the wall and at the free stream. Figure 13 and figure 14 depicts the effect of parameter (A) and (B) on Temperature field respectively. Both figures share similar characteristics as both figure shows a decrease in temperature from the wall and away from the wall, meanwhile at the free stream, there is a significant increase in the temperature of the fluid. Figure 15 shows the effect of Second-Grade parameter (α_0) on Temperature field. The figure shows a decrease in temperature away from the wall and an increase in the temperature of at the free stream. Figure 16 indicates the effect of Stretching Sheet parameter (λ) on Temperature field. It is revealed from the figure that the increasing effect of the parameter leads to a decrease in temperature away from the wall and an increase in the temperature of at the free stream. Figure 17 shows the effect of Pressure Gradient parameter (G) on Temperature field. Observation shows from the figure that temperature of the fluid increases at all point when there is an increasing effect of the Pressure Gradient.

Mass species (concentration) field

Mass species field describes the chemical processes, composition and quantities of substances. Figure 18 depict the effect of volume fraction (ϕ) on Concentration field. From the figure, the increase in the volume fraction parameter leads to the decrease in the concentration of the fluid at all point. Figure 19 indicates the effect of Hartmann number (Ha) on Concentration Field. It is a clear indication that the increase in the Hartmann number parameter would result in the significant increase in the concentration of the fluid. Figure 20 shows the effect of Soret Number (Sr) on Concentration field. The concentration of the fluid increases with the increase in the Soret number parameter. Figure 21 shows the effect of Buoyancy parameter (Gr) on Concentration field. From the figure, the increasing effect of Buoyancy parameter brings about the increase in the concentration of the fluid. Figure 22 shows the effect of Chemical reaction parameter (Ω) on Concentration field. It is revealed from the figure that the increase in the chemical reaction parameter yields an increase in the concentration of the fluid. Figure 23 represents the effect of radiation parameter (R) on Concentration field. The figure shows a slight decrease in the fluid concentration when there is an increase in the radiation parameter. Figure 24 represents the effect of Stretching Sheet parameter (λ) on Concentration field. It is seen in the figure that when there is an increase in the stretching sheet parameter, the fluid concentration decreases slight at all point. Figure 25 and figure 26 portraits the Effect of (A) and (B) on Concentration field respectively. From both figures, it is observed that the increase in the parameters leads to a slight decrease in the concentration of the fluid. Then Figure 27 shows the effect of

reaction index (r) on the mass species field. It is observed from the figure that the increase in the parameter results in a slight increase in the concentration field of the fluid.

Table 2 shows the effect of nanofluid Volume Fraction effect on the flow field (skin friction, Nusselt number and Sherwood number). It is observed from the table that the increase in the volume fraction $\phi = 0.0, 0.2$ yields an increase in the skin friction coefficient $f''(0)$ and at $\phi = 0.4$ it causes a decrease in the skin friction. This is also observed in the case of the wall temperature transfer $g'(0)$, meanwhile, the wall mass transfer $h'(0)$ decreases as the volume fraction $\phi = 0.0, 0.2, 0.4$. Table 3 shows the Variation of reactivity parameter (Ω), reaction index (r), second grade fluid parameter (α_0), unsteadiness parameter (β) with wall rate transfer and sheet stretching parameter (λ) It is observed from the table that the increase in the reactivity parameter (Ω) causes an increase at the wall rate transfer, the increase in the reaction index brings about the increase in the skin friction coefficient $f''(0)$, wall temperature gradient $g'(0)$ and the mass transfer $h'(0)$. With the increase in the second-grade fluid parameter (α_0) and the sheet stretching parameter (λ), the skin friction coefficient $f''(0)$, wall temperature gradient $g'(0)$ and the mass transfer $h'(0)$ decreases

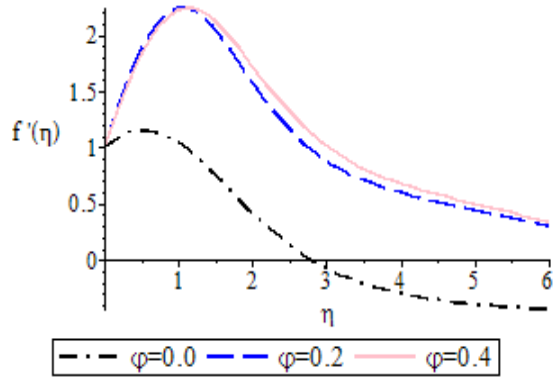

Fig.2: Effect of volume fraction (φ) on velocity field.

Table 3: Buoyancy force (Gr), Space/Temperature Dependent Heat Source/Sink $(\boldsymbol{A}\ and\ \boldsymbol{B})$ parameter, stretching sheet parameter $(\boldsymbol{\lambda})$, Hartmann number $(\boldsymbol{Ha})$ and the Darcy-Forcheimer parameter $(\boldsymbol{Fs})$ with wall rate transfer.

Parameter $(Gr, Nb, Nt, Sr, L$	C_f	Nu	Sh
Gr			
0.0	1.893902	1.320403	-1.281051
0.5	2.137235	1.514200	-1.100742
1.0	2.390207	1.732480	-0.864754
A* and *B			
0.2	2.132916	1.509235	-1.149395
0.4	2.119394	0.805233	-1.263327
0.6	2.111693	0.525512	-1.305991
λ			
0.2	2.135146	1.512137	-1.149599
0.4	2.120730	0.775143	-1.467782
0.6	2.101336	0.474465	-1.727259
Ha			
0.0	2.132357	1.472765	-1.290596
0.3	2.136222	1.470022	-1.047256
0.6	2.118973	1.440154	-0.813055
Fs			
2.0	2.129640	1.470657	-1.290698
4.0	2.133363	1.472626	-1.290445
6.0	2.129717	1.464886	-1.289977

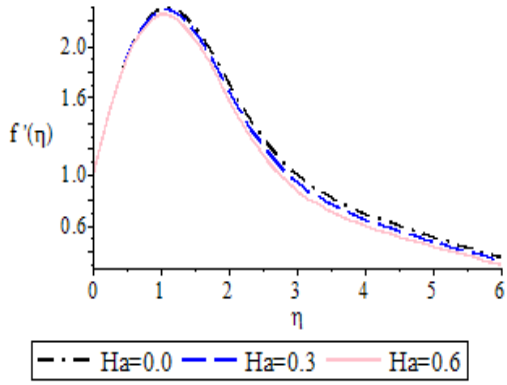

Fig.3: Effect of Hartman Number (Ha)on the velocity field.

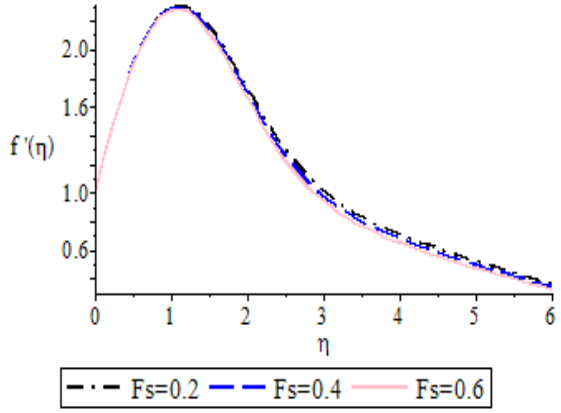

Fig. 4: Effect of Darcy Foreichemer parameter (Fs) on velocity field.

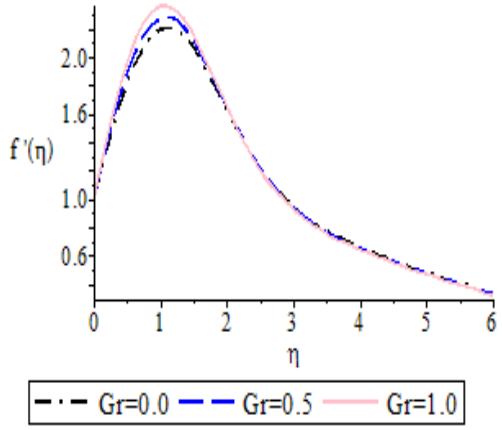

Fig.5: Effect of Buoyancy Parameter (Gr) on velocity field.

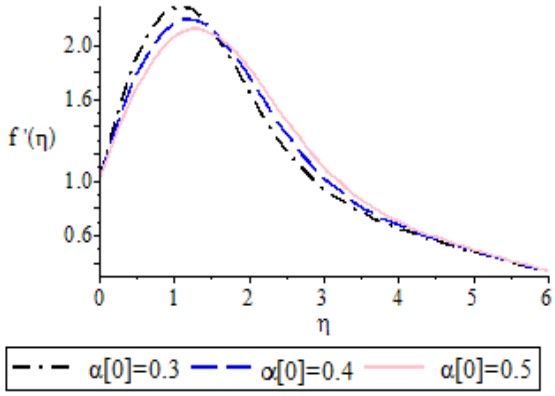

Fig.6: Effect of Pressure Gradient parameter (G) on velocity field.

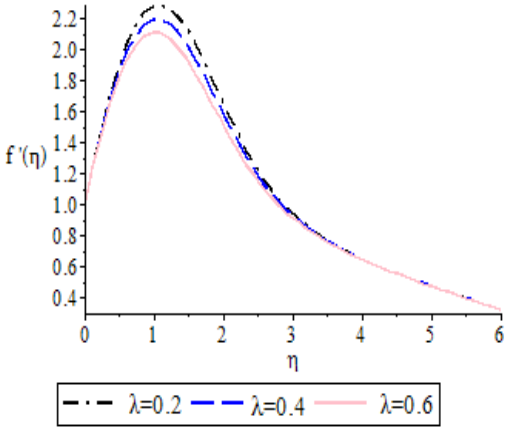

Fig.7: Effect of Stretching sheet parameter (λ) on velocity field.

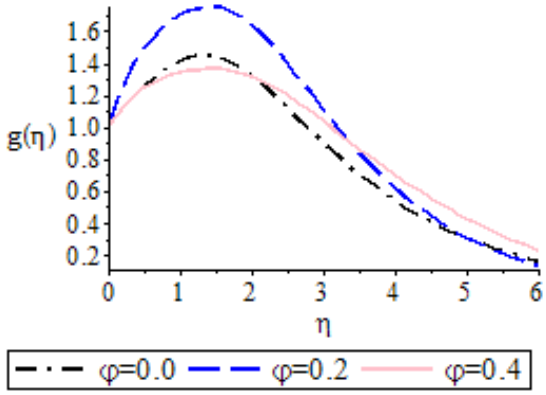

Fig.8: Effect of volume fraction (φ) on Temperature field.

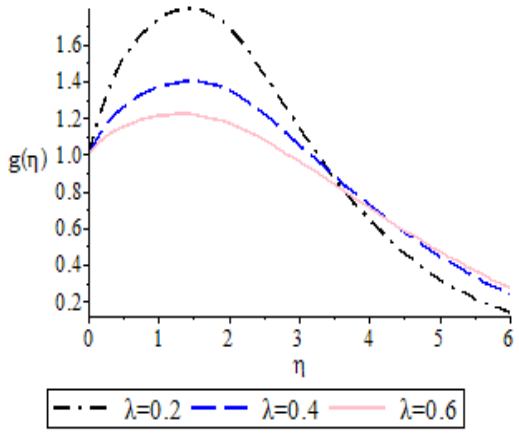

Fig.9: Effect of Stretching sheet parameter (λ) on Temperature field.

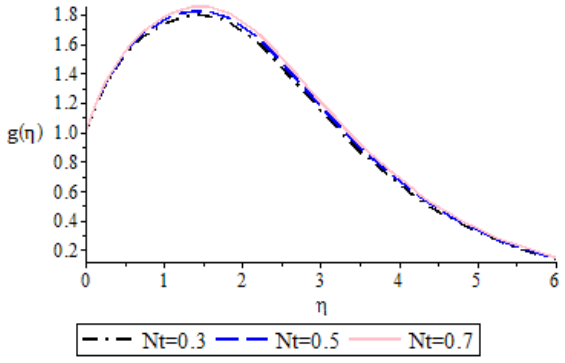

Fig. 10: Effect of Thermophoresis parameter (Nt) on Temperature field.

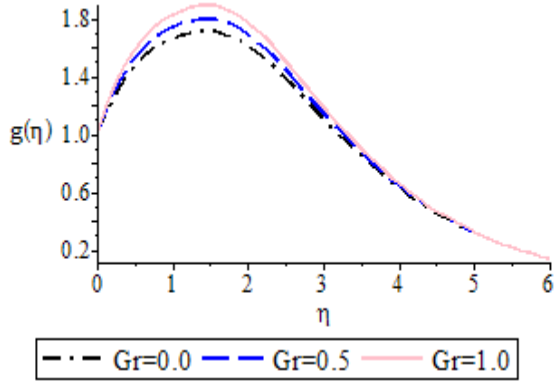

Fig.11: Effect of Buoyancy parameter (Gr) on Temperature field.

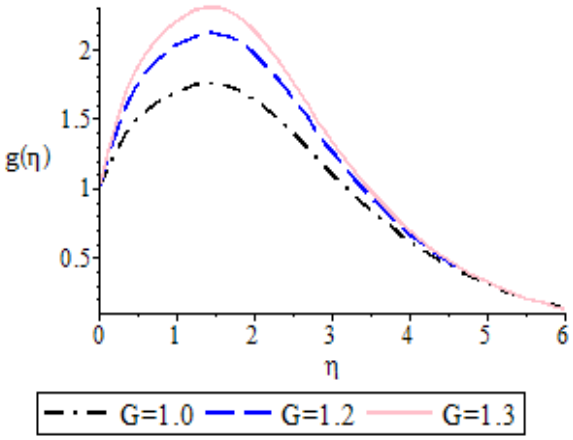

Fig.12: Effect of Pressure Gradient parameter (G) on Temperature field.

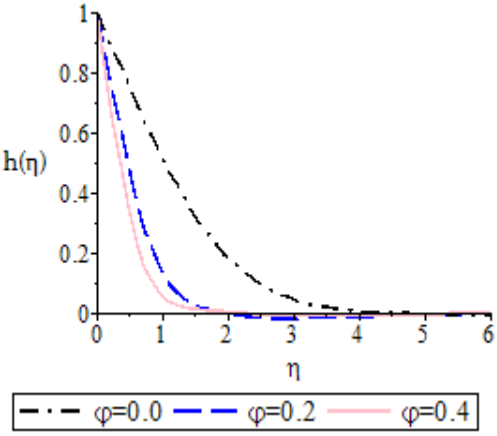

Fig.13: Effect of volume fraction (ϕ) on Concentration field.

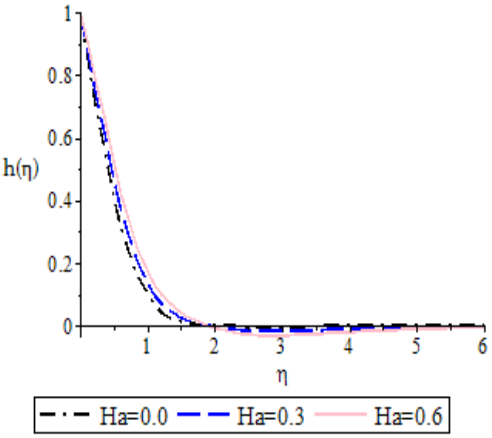

Fig.14: Effect of Hartmann number (Ha) on Concentration Field.

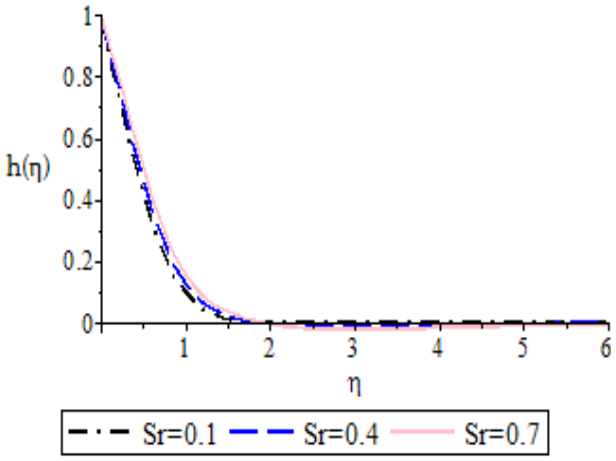

Fig. 15: Effect of Soret Number (Sr) on Concentration field.

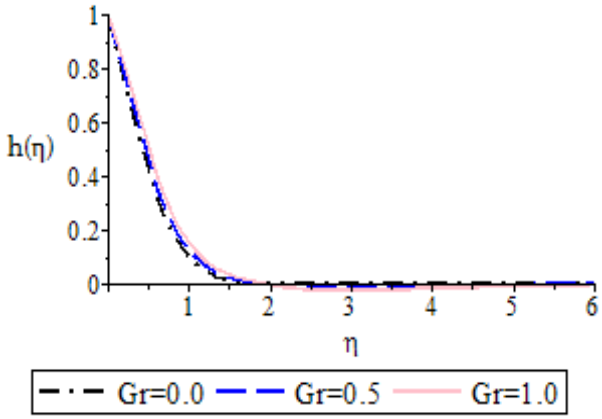

Fig.16: Effect of Buoyancy parameter (Gr) on Concentration field.

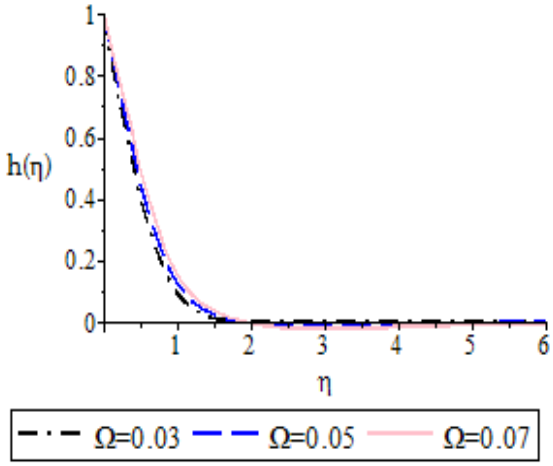

Fig.17: Effect of Chemical reaction parameter (Ω) on Concentration field.

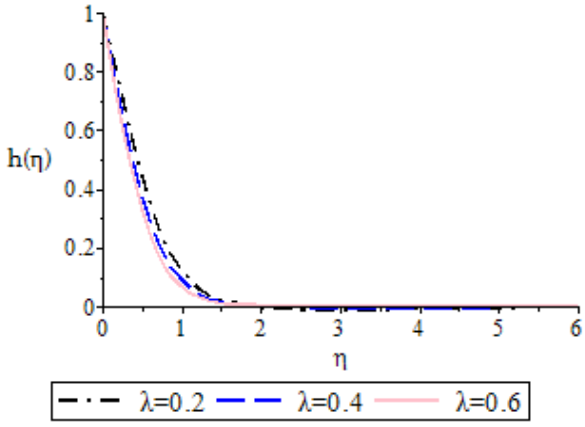

Fig.18: Effect of Stretching Sheet parameter (λ) on Concentration field.

4. CONCLUSION

This resaerch "Analysis of the Effects of Cu-Water Nanofluid Volume Fraction, Space/Temperature Dependent Heat Source/Sink on Magnetohydrodynamics (MHD) Heat and Mass Transfer of Stretching sheet with Buoyancy Forces", has been analysed extensively. The various controlling parameters shows the characteristics properties of the fluid under consideration. From the study, the following conclusion is drawn;

1. The increase in the volume fraction leads to an increase in the velocity field and a decrease in the temperature of the fluid of the fluid, meanwhile, an increase in the volume fraction leads to the decrease in the concentration of the fluid at all point and the increase and the increase in the Hartman number results to the decrease in the movement of the velocity field and an increase in the temperature and mass concentration of the fluid.

2. The increase in the porous medium causes a decrease in the velocity of the fluid. Also, the increase in the Buoyancy force leads to the increase in the motion of the fluid. Also, the pressure gradient is described as the rate of change of pressure with respect to

distance. This usually brings about the increase in the motion of fluid in a specific direction. This is shown in this study.

3. The temperature at all point increases when there is an increase in the Thermophoresis parameter and the Buoyancy forces. On the other hand, the increase in the radiation parameter leads to the decrease in the temperature of the fluid and the increase in the Eckert Number parameter shows yields a significant increase away from the wall and at the free stream.

4. The increase in the space/temperature heat source/sink brings about a decrease in temperature at some point and an increase at some other point. Also, a decrease in temperature away from the wall and an increase in the temperature of at the free stream occurs when there is an increase in the buoyancy force.

5. The increasing effect of the stretching sheet leads to a decrease in temperature away from the wall and an increase in the temperature at the free stream and that temperature of the fluid increases at all point when there is an increasing effect of the Pressure Gradient.

6. The concentration of the fluid increases with the increase in the Soret number. Meanwhile, the increasing effect of Buoyancy force brings about the increase in the concentration of the fluid and the increase in the chemical reaction parameter yields an increase in the concentration of the fluid.

7. There is a decrease in the fluid concentration when there is an increase in the radiation, an increase in the stretching sheet parameter causes the fluid concentration to decrease at all point and the increase in the reaction index results in increase in the concentration field of the fluid.

REFERENCES

Bijjanal J. G., Govinakovi S. R. and Channabasappa S. B. (2011). "Boundary Layer Flow of an Unsteady Dusty Fluid and Heat Transfer over a Stretching Sheet with Non-Uniform Heat Source/Sink". *ScientificResearch*, 3, 726-735. Doi:10.4236/eng.2011.37087

Anjali Devi S. P. and Agneeshwari (2019). "Effects Non-Uniform Heat Generation/Absorption and Radiation on Hydromagnetic Dissipative Flow over a Porous Nonlinear Stretching Surfacewith Heat and Mass Fluxes". *International Journal of Applied Mechanics and Engineering.* Vol.24, no. 4, pp.36-52. DOI: 10.2478/ijame-2019-0048

Choi, S. (1995). Enhancing thermal conductivity of fluids with nanoparticles. In D. A. Siginer & H. P. Wang (Eds.), *Development and applications of non-Newtonian flows* (pp. 99-105). New York: ASME Press.

Chon CH, Kihm KD, Lee SP and Choi SUS (2005) "Empirical correlation finding the role of temperature and particle size for nanofluid (Al_2O_3) thermal conductivity enhancement" *Appl. Phys. Lett.* 87 (97), 153107.

Liu M, Lin MC and Wang C. (2011) "Enhancements of thermal conductivities with Cu, CuO, and carbon nanotube nanofluids and application of MWNT/water nanofluid on a water chiller system." *Nanoscale Research Letter* 6, 297. doi:10.1186/1556-276X-6-297.

Kwak K and Kim C. (2005) "Viscosity and thermal conductivity of copper oxide nanofluid dispersed in ethylene glycol." *Korea-Australia Rheology Journal*. *17*, 35–40.

Animasaun IL and Sandeep N (2016) "Buoyancy induced model for the flow of 36 nm alumina-water nanofluid along upper horizontal surface of a paraboloid of revolution with variable thermal conductivity and viscosity" *Power Technology* **301**, 858 - 867. doi: /10.1016/j.powtec.2016.07.023

Abu-Nada E (2009) "Effects of variable viscosity and thermal conductivity of Al_2O_3water nanofluid" *Int. J. Heat Fluid Flow* (2009), doi: 10.1016/j.ijheatfluidflow.2009.02.003.

Angue M, Roy HG, Nguyen CT and Doucet D (2009) "New temperature and conductivity data for water-based nanofluids". *Int. J. Therm. Sci. 48* (2), 363–371,

Makinde OD and Animasaun IL

(2016) "Bioconvection in MHD nanofluid flow with nonlinear thermal radiation and quartic autocatalysis chemical reaction past an upper surface of a paraboloid of revolution," *International Journal of Thermal Sciences* **109**, 159 - 171.

Kannaiyan S, Boobalan C, Umasankaran A, Ravirajan A, Sathyan S, and Thomas T (2017). Comparison of experimental and calculated thermophysical properties of alumina/cupric oxide hybrid nanofluids. *Journal of Molecular Liquids*, 244, 469-477. doi: 10.1016/j.molliq.2017.09.035

Nguyen CT, Desgranges F, Roy G, Galanis N, Mare T, Boucher S and Angue Minsta H, "Temperature and particle-size dependent viscosity data for water based nanofluids – hystresis phenomenon". *Int. J. Heat Fluid Flow* 28, 1492–1506 (2007).

Ahmad B. J., Sharidan S., Imran U., Rabia S., Wasim J., Amjad A. P., Mustafa M. R., Syed M. H., Aysha R., Elsayed M. T. and Mohamed R. E.(2022) "Mixed Convective Flow of an Electrically Conducting Viscoelastic Fluid Past a Vertical Nonlinearly Stretching Sheet", *Scientific reports,* https://doi.org/10.1038/s41598-022-18761-0.

Buongiorno J. (2006), "Convective transport in nanofluids", *Journal of Heat Transfer* 128 (2006) 240–250.

Hatem G., Umair K., Aurang Z., Anuar I., Sayed M. E. and Zehba R. (2022)" analysis of mixed convection on two-phase nanofluid flow past a vertical plate in Brinkman-extended darcy porous medium with nield condition" *mathematics* https://doi.org/10.3390/math10203918.

Mohsen S. and Davood D. G. (2016), "External Magnetic Field Effects on Hydrothermal Treatment of Nanofluid", *Elsevier*, page 1 – 47, https:doi.org/10.1016/B978-323-43138-5.00001-x

Okedoye A. M and Akinrinmade V. A. (2017), "Analysed the MHD Mixed Convection Heat and Mass Transfer Flow from Vertical Surfaces in Poros Media with Soret and Dufour Effects" *Journal of Scientific and Engineering Research,* 4(9):75-85, www.jsaer.com.

Sathy S., Shanthi S. R. and Mamatha S. U. (2022), "Micro and Nanofluid Convective with Magnetic field Effects of Heat and Mass Transfer Applications Using MATLAB" *International Journal of Modern Physics*, page 133-151, https://doi.org/10.1016/B978-12-823140-1.00002-6

Shizhi *etal* (2012), "Applications of magnetohydrodynamics (MHD) in microfluid, handbook: chemistry, physics and life science principles (1st edition). CRC press, ISBN9780429093388, https://doi.org/10.1201/b11377.

Vyacheslav chernyshev (2010), "International Coorperation in MHD Electrical Power Generation", *IAEA Division of nuclear power and reactor*, IAEA BULLETIN. **VOL.20**, NO. 1